Materials Science and Engineering B 111 (2004) 101–106

www.elsevier.com/locate/mseb

Structure and magnetic properties in the compounds of $Sr_2FeMo_{1-x}Nb_xO_6$

X. Zhao [a,b], R.C. Yu [a,*], Y. Yu [a], F.Y. Li [a], Z.X. Liu [a], G.D. Tang [b], C.Q. Jin [a]

[a] *Key Laboratory of Extreme Conditions Physics, Institute of Physics, Center for Condensed Matter Physics, Beijing High Pressure Research Center, Chinese Academy of Sciences, P.O. Box 603, Beijing 100080, PR China*

[b] *Department of Physics, Hebei Normal University, Shijiazhuang 050016, Hebei, PR China*

Received 30 June 2003; accepted 21 March 2004

Abstract

The series of the $Sr_2FeMo_{1-x}Nb_xO_6$ compounds have been synthesized throughout the range of $0 \leq x \leq 1$ using conventional solid-state reaction method. The compounds show a tetragonal structure in the range of $0 \leq x \leq 0.4$ while showing an orthorhombic structure in the range of $0.5 \leq x \leq 1$. Magnetic and electrical properties of the compounds have been studied in order to investigate the effect of the substitution of non-magnetic Nb^{5+} ion for Mo^{5+} (or Mo^{6+}) ion in the double perovskite compound. The magnetization (M) values are found to decrease slowly with increasing x in all compounds with $0 \leq x \leq 0.75$ due to less correlation among the magnetic ions induced by the non-magnetic Nb^{5+} ions. The measurements of magnetic susceptibilities at zero-field-cooled and field-cooled conditions show that a transition from a ferromagnetic (FM) to a ferro-cluster glass state gradually transforms from a paramagnetic (PM) to a spin-glass state with increasing Nb^{5+} content. With increasing x, the conductivity decreases. Meanwhile, the compounds lose the ferromagnetic component. The compounds have good conductivity from 10^{-3} to 10 Ω cm with x in the range of $0 \leq x \leq 0.3$, though they show insulator behavior. While those with x in the range of $0.6 \leq x \leq 0.75$ show poor transport property. All samples with $x \geq 0.25$ show large negative magnetoresistances (MRs), similar to that observed in Sr_2FeMoO_6.

Keywords: Substitution; $Sr_2FeMo_{1-x}Nb_xO_6$; Double perovskite; Clossal magnetoresistance

1. Introduction

Recently, large negative magnetoresistance (MR) was reported in the Sr_2FeMoO_6 double perovskite [1]. Ordered Sr_2FeMoO_6 has alternating occupancies of Fe and Mo ions at B sites of perovskite ABO_3 structure, where A and B represent two different cations. Sr_2FeMoO_6 is known as a ferrimagnet metal with a very high ferromagnetic (FM) transition temperature [1,2]. Each B-site sublattice of Fe^{3+} ($3d^5$) and Mo^{5+} ($4d^1$) arranges ferromagnetically, while the two sublattices are coupled anti-ferromagnetically. The $3d^5$ electrons of Fe^{3+} ions are localized showing local spin moment $S = 5/2$, while the $4d^1$ electrons of Mo^{5+} occupy the conduction band showing spin moment $S = 1/2$ on opposite direction. Up to now, there is still uncertainty about the mechanism for the magnetic interaction in this compound. The saturation magnetization value reported in [1] suggests the configuration of either $3d^5(Fe^{3+})$ and $4d^1(Mo^{5+})$ or $3d^6(Fe^{2+})$ and $4d^0(Mo^{6+})$. Many groups have done research work on magnetism for this compound [3–8]. Mössbauer spectroscopy studies [6] gave more reliable information of Fe^{3+} configuration. The configuration of $Fe^{2+}Mo^{6+}$ should be given with great care since the compound is a metal. Some neutron diffraction measurements [4] gave $0.5\mu_B$ for Mo while some [3] reported zero for it. Considering electronic itineracy of Mo spin down t_{2g} electrons is compellent to explain the saturation magnetization and the conductivity of the compound. Besides these, cationic disorder of the Fe and Mo sites with a few percent might also play a significant role in the nature of the magnetism [9,10]. It has been suggested that Sr_2FeMoO_6 compound has a half-metal ferromagnetic (HMFM) state, where only minority spins are present at the Fermi level. Thus, only one kind of the spin polarized electrons serves the conductivity.

* Corresponding author. Tel.: +86-1-82649159; fax: +86-1-82649531.
E-mail address: rcyu@aphy.iphy.ac.cn (R.C. Yu).

0921-5107/$ – see front matter © 2004 Elsevier B.V. All rights reserved.
doi:10.1016/j.mseb.2004.03.021

This compound exhibits a large negative MR at 5 K as well as at 300 K. It is also reported that a disorder between the Fe and Mo occupancies destroys the HMFM state and as a consequence the CMR effect also decreases [11]. Recently magnetic and electrical properties have been investigated in $Sr_2FeMo_{1-x}W_xO_6$ [12–14], $Sr_2Fe_{1-x}Cr_xMoO_{6-y}$ [15], $Sr_{2-x}Ba_xFeMoO_6$ [16–18], $Sr_2FeMoO_{6+\delta}$ [19], etc. [20]. As is well known, Sr_2FeNbO_6 shows very different structural and physical properties without showing the ordering of the cations Fe^{3+} and Nb^{5+} over the six-coordinate sites of the perovskite structure. Sr_2FeNbO_6 is an anti-ferromagnetic (AFM) insulator throughout the whole temperature range with T_N of 25 K, where the magnetic moments of Fe^{3+} ions show anti-ferromagnetic interactions at low temperature [21]. Sr_2FeNbO_6 contains Nb^{5+} ($4d^0$) and Fe^{3+} ($3d^5$) species where Nb^{5+} is a non-magnetic ion. In view of the $4d^0$ electronic configuration of Nb^{5+}, the Fe^{3+} ions are believed to couple anti-ferromagnetically with each other via super-exchange interaction. Since Sr_2FeMoO_6 and Sr_2FeNbO_6 have different structures and magnetic properties, it is meaningful to study the structures and physical properties of $Sr_2FeMo_{1-x}Nb_xO_6$ and the effect of non-magnetic Nb^{5+} ion in the compounds. This will be helpful for further understanding the CMR effect in double perovskite-like compounds.

2. Experiments

The polycrystalline samples of the series of $Sr_2FeMo_{1-x}Nb_xO_6$ compounds were prepared by using a traditional solid-state reaction method. The stoichiometric mixtures of $SrCO_3$, Fe_2O_3, MoO_3, and Nb_2O_5 were first calcined at 1000 °C for 4 h in a flow of Ar gas, and then mixed thoroughly in an agate mortar and pressed into pellets. The pellets were sintered at 1100 °C for 3 h in a 1% H_2/Ar flow, and finally at a temperature of 1125 °C for 16 h with several intermediate grindings. The detailed procedure of sample preparation was described elsewhere [22]. The room temperature X-ray diffraction (XRD) measurements were performed using a Rigaku D/Max-2400 diffractometer with Cu Kα radiation. Magnetic moment and resistivity versus temperature were measured using a Mag Lab System (2000 Oxford UK). Resistivity was measured with the four-probe technique. Samples were cut into a rectangular shape with approximate dimensions 8 mm × 3 mm × 1.5 mm. Electrical contacts were established using silver paint. The morphology observation and composition analysis were carried out with XL30 S-FEG scanning electron microscope (SEM) equipped with energy dispersive analysis of X-ray (EDAX).

3. Results and discussion

Fig. 1 shows the XRD patterns for the $Sr_2FeMo_{1-x}Nb_xO_6$ samples. No impurity is detected in the series of the samples,

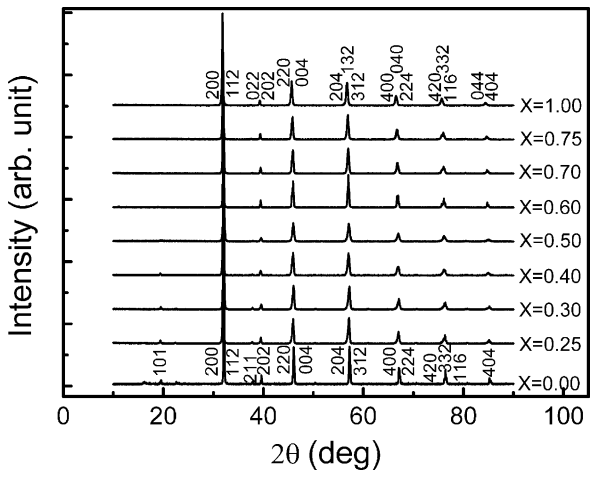

Fig. 1. X-ray diffraction patterns of $Sr_2FeMo_{1-x}Nb_xO_6$ samples. No impurity is detected in all the samples. The samples with $x \leq 0.4$ have a tetragonal structure, while those with $x \geq 0.5$ have an orthorhombic one.

indicating well-substituted compounds. In the XRD patterns for $x = 0$–0.4 samples, there is a small super-lattice peak at $2\theta \sim 19°$, which is the characteristic of ordered state in the double perovskite structure. The XRD patterns for the samples with x in the range of 0–0.4 can be indexed to a tetragonal structure with a space group *I*4/*mmm*. The XRD patterns for $x = 0.5$–1.0 show no existence of the super-lattice peak at $2\theta \sim 19°$ and they can be indexed to an orthorhombic structure with a space group *Pnma*. The indexes of the structures are shown in the patterns.

Table 1 presents the lattice parameters and unit cell volumes at different compositions. The lattice constants and the cell volumes increase with increasing Nb content. But they do not follow the rule in the range between 0.4 and 0.5 due to the structural transition from the tetragonal to the orthorhombic structure. This transition is also accompanying the order–disorder transition in the structure.

Temperature dependence of magnetization (*M*) for $Sr_2FeMo_{1-x}Nb_xO_6$ is presented in Fig. 2. In the range of $0.25 \leq x \leq 0.5$, with increasing temperature the compounds first undergo a magnetic transition from an anti-ferromagnetic (AFM) to a ferromagnetic state at lower temperature and then to a paramagnetic (PM) state at higher

Table 1
Lattice parameters and volumes with different compositions

Nb content, *x*	*a* (Å)	*b* (Å)	*c* (Å)	*V* (Å^3)
0	5.568(3)		7.878(7)	244.2(3)
0.25	5.570(2)		7.875(4)	244.3(2)
0.30	5.591(5)		7.90(2)	247.1(4)
0.40	5.59(2)		7.92(3)	247.6(6)
0.50	5.55(4)	5.62(4)	7.87(2)	245.5(6)
0.60	5.61(3)	5.62(3)	7.88(2)	248.5(4)
0.70	5.60(3)	5.63(3)	7.89(2)	248.5(4)
0.75	5.61(2)	5.62(2)	7.907(8)	249.5(3)
1.00	5.617(4)	5.614(2)	7.952(4)	250.7(2)

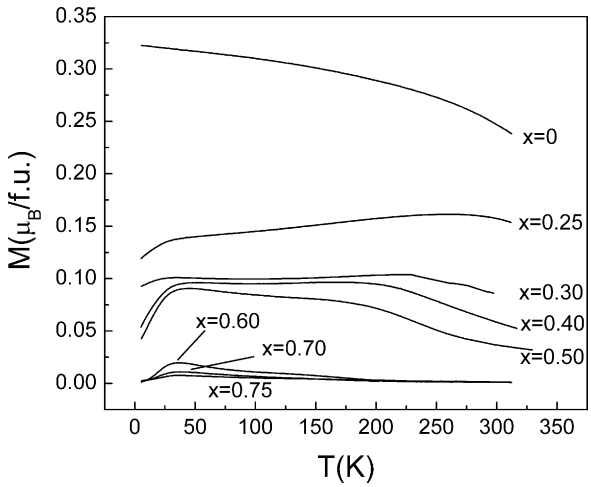

Fig. 2. Magnetization vs. temperature curves for $Sr_2FeMo_{1-x}Nb_xO_6$ at 0.01 T.

temperature. With increasing x, the magnetization value of the sample reduces gradually and the transition temperature (T_C) from the FM to PM decreases, which shows the expense of ferromagnetic state. This shows that there is competition between the FM and AFM interactions with increasing Nb content. When x is up to 0.6, the magnetic phase transition from FM to PM state disappear and the magnetization decreases remarkably. It can be seen from Fig. 2 that the M–T curve for $x = 0.75$ is very close to that for $x = 0.7$ though it shows lower values. The anti-ferromagnetic transition temperature (T_N) was around 35 K with minor variation, and in agreement with a reported value of 25 K. The T_C and/or T_N of the $Sr_2FeMo_{1-x}Nb_xO_6$ compounds are presented in Table 2 in order to give a clear comparison. These properties are different from the $Sr_2FeMo_{1-x}W_xO_6$ system [12], where the M–T curves show a cusp or broadened peak feature around 50 K with a minimal variation of peak temperature. However, some characters are similar to the case of $Pr_{0.5}Sr_{0.5}Mn_{1-x}M_xO_3$ (M = Ga, In, Al or M = Ti, Sn) [23], where the T_C also decreases with increasing x in the range of 0–0.06 for M = Ga, In and 0–0.08 for M = Ti, Sn. The T_N increases and merges with T_C finally with increasing x in the case of M = trivalent cations, while the anti-ferromagnetic state tends to be destroyed with increasing x in the case of M = tetravalent cations. But in our experiments, the T_N of $Sr_2FeMo_{1-x}Nb_xO_6$ almost keeps the same value with increasing Nb content.

Table 2
T_C and/or T_N of the $Sr_2FeMo_{1-x}Nb_xO_6$ compounds with different compositions

Nb content, x	T_N (K)	T_C (K)
0		415
0.25	34	406
0.30	33	403
0.40	38	395
0.50	40	380
0.60	36	
0.70	38	
0.75	36	

The possible scenarios to explain these observed results are to reduce ferromagnetic coupling and increase the anti-ferromagnetic coupling between Fe^{3+} by the substitution of non-magnetic Nb^{5+} for Mo^{5+}(or Mo^{6+}) ion. Thus, the $Sr_2FeMo_{1-x}Nb_xO_6$ behaves in a ferromagnetic state macroscopically in the compounds with less content of non-magnetic Nb^{5+} ions and in an anti-ferromagnetic state in those with more contents of Nb^{5+}. The magnetization value decreases by increasing the substitution of Nb for Mo. It needs to be noted that the vanishment of the ferromagnetic state in the range of $0.5 \leq x \leq 0.6$ is probably accompanied with the structural transition from the tetragonal to the orthorhombic structure, which is shown in Fig. 1 as well as in Table 1. Here, it should be pointed out that the composition range corresponding to the vanishment of the ferromagnetic state is a little higher than those corresponding to the structural transition.

Since the vanishment of the ferromagnetic state occurs in the range of $0.5 \leq x \leq 0.6$, we take the compounds with $x = 0.4, 0.5, 0.6, 0.7$ as the candidates for the following measurements. Fig. 3 shows the temperature dependence of the magnetization for $Sr_2FeMo_{1-x}Nb_xO_6$ ($x = 0.4, 0.5, 0.6, 0.7$) measured after cooling in the zero magnetic field (ZFC) and after cooling in a magnetic field (FC). From thermo-magnetization of typical samples in the processes of ZFC and FC warming runs, we can observe a considerable deviation in temperatures below FM–PM transition, and the deviation decreases with increasing Nb content. This large thermo-magnetic irreversibility suggests a ferro-cluster-glass in the compounds, which might be caused by the competition between the FM and AFM interactions. For $x = 0.4$ and 0.5, the samples still exhibit FM from 35 to 205 K and from 35 to 190 K, respectively, and change to AFM state below 35 K. While for $x = 0.6$ and 0.7, a clear

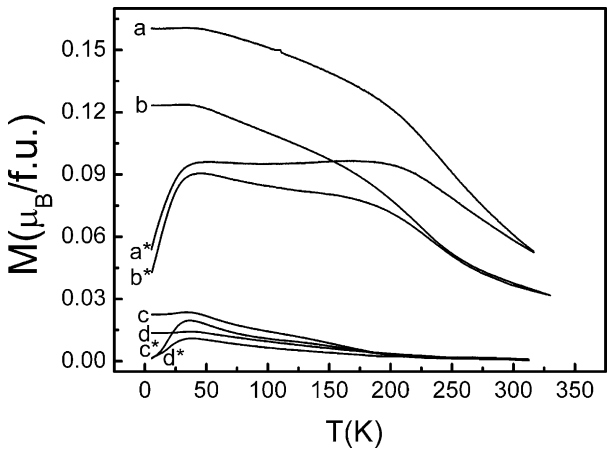

Fig. 3. Temperature dependence of magnetization for $Sr_2FeMo_{1-x}Nb_xO_6$. a* and a, b* and b, c* and c, and d* and d are the M–T curves at ZFC and FC under an applied field of 0.01 T for $x = 0.4, 0.5, 0.6, 0.7$, respectively.

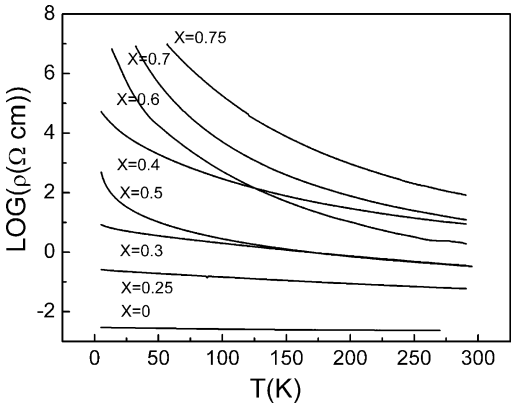

Fig. 4. Resistivity vs. temperature curves for polycrystalline $Sr_2FeMo_{1-x}Nb_xO_6$ at zero magnetic field.

cusps occur in both FC and ZFC magnetization measurements, indicating a spin-glass state. This is similar to the case in Sr_2FeNbO_6 where the spin-glass state occurs at low temperature [21]. Those ZFC and FC measurements show that with increasing x, the transition from PM to FM state first transforms from PM to ferro-cluster glass and further to AF state, and finally from PM to spin-glass state as the temperature decreases. These results are in good agreement with the reduction of magnetic moment by increasing the content of non-magnetic Nb^{5+} ions.

The electrical resistivities (ρ) versus temperature for the samples are presented in Fig. 4 with a logarithmic scale as a function of temperature. All of the samples exhibit an insulating or semi-conducting behavior. Evidently, ρ versus temperature plots clearly demarcate two regimes. The compounds with $x \leq 0.3$ have low resistivities from 10^{-3} to $10\,\Omega\,cm$, though they exhibit an insulating or semi-conducting behavior, while those with $x \geq 0.6$ have high resistivities. It is interesting that the compounds with $x = 0.5$ has lower resistivity and higher change rate versus temperature than those with $x = 0.4$. This is caused by order–disorder transition accompanying the structural change from the tetragonal to the orthorhombic phase. Due to the same structural type of the compounds with $x \geq 0.5$, the resistivities of the compounds increase and exhibit nearly the same changing rate versus temperature with increasing the Nb content. Thus, these results clearly establish a transition of the resistivity change rate versus temperature as a function of Nb content in the region of $0.4 \leq x \leq 0.6$. The behavior of electrical resistivity in $Sr_2FeMo_{1-x}Nb_xO_6$ with increasing Nb content is similar to that in $Sr_2FeMo_{1-x}W_xO_6$ system [14], i.e., resistivity value increases with increasing x over the whole Mo composition range. However, all of the samples in $Sr_2FeMo_{1-x}Nb_xO_6$ show an insulating or semi-conducting behavior in our experiments, while the samples in $Sr_2FeMo_{1-x}W_xO_6$ system exhibit a change from insulator to metal with decreasing W content.

The resistivity has very close relationship with grain boundary and grain size. At both sides of the structural transition composition, four samples were chosen for SEM observation and composition analysis. Fig. 5(a)–(d) show the SEM morphologies of the samples with $x = 0.25$, 0.4, 0.5 and 0.7, respectively. Four samples have nearly same size grains and nearly same grain boundary case. The compositions of the samples obtained by EDAX measurement in situ SEM are very close to the nominal ones. These results suggest that different resistivity behaviors of the samples are caused by the different chemical compositions, not by the grain size and grain boundaries.

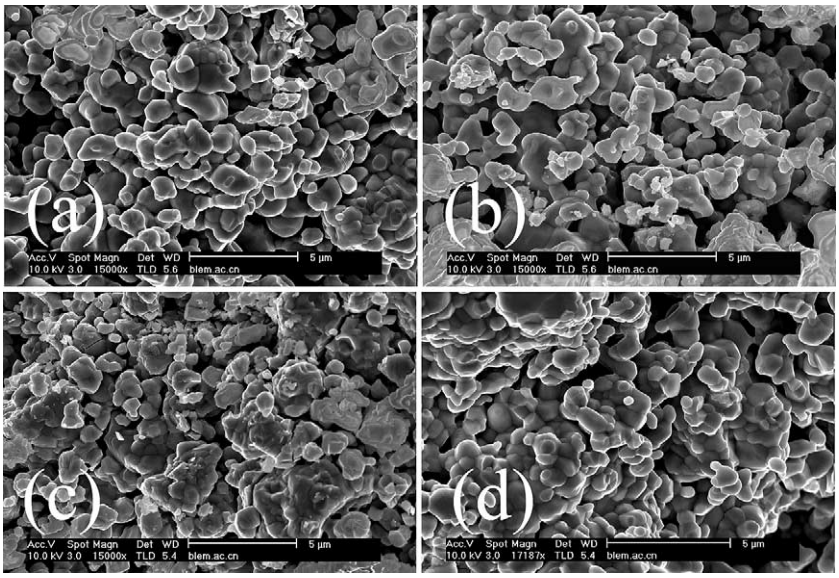

Fig. 5. SEM morphologies of the samples $Sr_2FeMo_{1-x}Nb_xO_6$ with: (a) $x = 0.25$, (b) $x = 0.4$, (c) $x = 0.5$, and (d) $x = 0.7$.

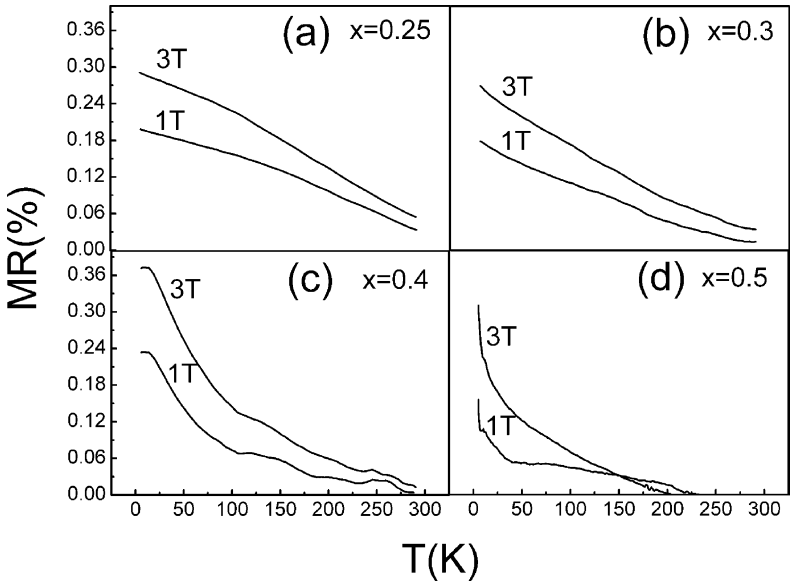

Fig. 6. Temperature dependence of magnetoresistance values for $Sr_2FeMo_{1-x}Nb_xO_6$ at 1 and 3 T: (a) $x = 0.25$; (b) $x = 0.3$; (c) $x = 0.4$; and (d) 0.5.

As is known, the Sr_2FeMoO_6 has a ferromagnetic arrangement. With the substitution of non-magnetic Nb^{5+} ions for Mo ions, the neighboring Fe ions are intervened by the Nb^{5+} ions and the ferromagnetic arrangement is weakened, but the compounds with less substitution of Nb still show ferromagnetic character and good conductivity. With further substitution of Nb, the large scale ferromagnetic arrangement becomes ferro-clusters and some neighbor Fe ions have anti-ferromagnetic arrangement. As a consequence, the magnetization value decreases and the resistivity increases. With further substitution, the ferromagnetic clusters become smaller and the anti-ferromagnetic coupling between Fe ions are dominant. Finally the compounds show the anti-ferromagnetic behavior with high resistivities.

A magnetoresistance value can be calculated using the following definition:

$$\mathrm{MR}(T, H) = \frac{\rho(T, 0) - \rho(T, H)}{\rho(T, 0)} \times 100\%$$

where H denotes the external field and, $\rho(T,0)$ and $\rho(T, H)$ represent the resistivities at 0 and H fields, respectively. Due to the high resistivity of the compounds with high Nb content, we chose some compounds with low Nb content for the MR measurement. Fig. 6(a)–(d) present the temperature dependence of MR for the samples with $x = 0.25$, 0.3, 0.4, 0.5 at 1 and 3 T, respectively. For all the samples, the MR value increases smoothly with decreasing temperature, which shows a typical behavior of tunneling-type magnetoresistance. In $Sr_2FeMo_{0.6}Nb_{0.4}O_6$, at 5 K the MR values are as large as 23% (1 T) and 31% (3 T), respectively, and in $Sr_2FeMo_{0.75}Nb_{0.25}O_6$, the MR values are 4% (1 T) and 6% (3 T), respectively, at 290 K.

4. Conclusions

Magnetic and electrical properties as well as the MR have been investigated for the $Sr_2FeMo_{1-x}Nb_xO_6$ polycrystalline samples. The magnetization value decreases with increasing x due to less correlation among the magnetic ions induced by the non-magnetic Nb^{5+} ions. With increasing x, the transition from PM to FM state first transforms from PM to ferro-cluster glass further to AF state, and finally from PM to spin-glass state as the temperature decreases. All the samples show insulating or semi-conducting behavior in electrical transport property and the samples with $x = 0.4$ and 0.6 show large MR at 1 and 3 T similar to that observed in Sr_2FeMoO_6. For example, at 5 K $Sr_2FeMo_{0.6}Nb_{0.4}O_6$ exhibits MR values of 23 and 31% at 1 and 3 T, respectively. Furthermore, $Sr_2FeMo_{0.75}Nb_{0.25}O_6$ shows MR values of 4% (1 T) and 6% (3 T) at 290 K.

Acknowledgements

This work was supported by the National Natural Science Foundation of China (Nos. 10274099, 50321101 and 50332020) and the Sate key Development Project on Fundamental Research (No. 2002CB613301).

References

[1] K.-I. Kobayashi, T. Kimura, H. Sawada, K. Terakura, Y. Tokura, Nature 395 (1998) 677.
[2] T. Nakagawa, J. Phys. Soc. Jpn. 27 (1969) 880.
[3] B. García-Landa, C. Ritter, M.R. Ibarra, J. Blasco, P.A. Algarabel, R. Mahendiran, J. García, Solid State Commun. 110 (1999) 435.

[4] Y. Moritomo, Sh. Xu, T. Akimoto, A. Machida, N. Hamada, K. Ohoyama, E. Nishibori, M. Takata, M. Sakata, Phys. Rev. B 62 (2000) 14224.
[5] J. Lindén, T. Yamamoto, M. Karppinen, H. Yamauchi, T. Pietari, Appl. Phys. Lett. 76 (2000) 2925.
[6] A.W. Sleight, J.F. Weicher, J. Phys. Chem. Solids 33 (1972) 679.
[7] M. Venkatesan, M. Grafoute, A.P. Douvalis, J.-M. Greneche, R. Suryanarayanan, J.M.D. Coey, J. Magn. Magn. Mater. 242–245 (2002) 744.
[8] S.E. Lofland, T. Scabarozi, Y. Moritomo, Sh. Xu, J. Magn. Magn. Mater. 260 (2003) 181.
[9] A.S. Ogale, S.B. Ogale, R. Ramesh, T. Venkatesan, Appl. Phys. Lett. 75 (1999) 537.
[10] Y. Moritomo, H. Kusuya, A. Machida, T. Akimoto, Jpn. J. Appl. Phys. 39 (2000) L360.
[11] D.D. Sarma, E.V. Sampathkumaran, S. Ray, R. Nagarajan, S. Majumdar, A. Kumar, G. Nalini, T.N. Guru Row, Solid State Commun. 114 (2000) 465.
[12] K.-I. Kobayashi, T. Okuda, Y. Tomioka, T. Kimura, Y. Tokura, J. Magn. Magn. Mater. 218 (2000) 17.
[13] J. Lindén, T. Yamamoto, J. Nakamura, M. Karppinen, H. Yamauchi, Appl. Phys. Lett. 78 (2001) 2736.
[14] S. Ray, A. Kumar, S. Majumdar, E.V. Sampathkumaran, D.D. Sarma, J. Phys. Condens. Matter 13 (2001) 607.
[15] J. Blasco, C. Ritter, L. Morellon, P.A. Algarabel, J.M. De Teresa, D. Serrate, J. García, M.R. Ibarra, Solid State Sci. 4 (2002) 651.
[16] C. Ritter, M.R. Ibarra, L. Morellon, J. Blasco, J. García, J.M. De Teresa, J. Phys. Condens. Matter 12 (2000) 8295.
[17] T. Goko, Y. Endo, E. Morimoto, J. Arai, T. Matsumoto, Physica B 329 (2003) 837.
[18] J. Navarro, C. Frontera, D. Rubi, N. Mestres, J. Fontcuberta, Mater. Res. Bull. 38 (2003) 1477.
[19] D. Niebieskikwiat, A. Caneiro, R.D. Sánchez, J. Fontcuberta, Physica B 320 (2002) 107.
[20] C. Ritter, J. Blasco, L. Morellon, J.M. De Teresa, J. García, M.R. Ibarra, J. Magn. Magn. Mater. 226 (2001) 1070.
[21] K. Tezuka, K. Henmi, Y. Hinatsu, J. Solid State Chem. 154 (2000) 591.
[22] P. Zhao, Z.X. Bao, C.X. Liu, M.Z. Jin, R.C. Yu, C.Q. Jin, Chin. J. High Pressure 16 (2002) 137.
[23] A. Maignan, C. Martin, B. Raveau, Z. Phys. B 102 (1997) 19.